Dyes and Pigments 80 (2009) 287–291

Contents lists available at ScienceDirect

Dyes and Pigments

journal homepage: www.elsevier.com/locate/dyepig

The effects of Al and Ba on the colour performance of chromic oxide green pigment

Ping Li [a,b], Hong-Bin Xu [a,*], Yi Zhang [a], Zuo-Hu Li [a], Shi-Li Zheng [a], Yu-Lan Bai [c]

[a] Key Laboratory of Green Process and Engineering, Institute of Process Engineering, Chinese Academy of Sciences, Beijing 100190, PR China
[b] Graduate School of Chinese Academy of Sciences, Beijing 100039, PR China
[c] College of Science, Qingdao University of Agriculture, Qingdao 266109, PR China

ARTICLE INFO

Article history:
Received 11 March 2008
Received in revised form 8 July 2008
Accepted 22 July 2008
Available online 22 August 2008

Keywords:
Chromic oxide green pigment
Hydrogen reduction
Activated sintering
Colour performance
Phase composition
Microstructure

ABSTRACT

On the basis of the novel hydrogen reduction of chromite ore, an activated sintering method was devised to prepare chromic oxide green pigment. Using XRD, SEM, EDX, ICP-AES, UV and reflectance colorimetry it was found that the colour performance of the synthesized pigment was markedly improved by adding Al and Ba, which resulted in the formation of an Al_2O_3–Cr_2O_3 solid solution and a secondary $BaCr_2O_4$ phase, respectively, within the pigment. The colour performance of the chromic oxide green pigment doped with 0.1% Al and 0.55% Ba conformed to commercial pigment standards.

1. Introduction

Chromic oxide green pigment finds wide applications in ceramics, coatings, printing, gum elastic, plastics and construction materials due to its excellent performance in green colour, wear resistance, corrosion resistance, and chemical resistance.

At present, the industrial production of chromic oxide green pigment generally employs two technical routes: one is the reduction of $Na_2Cr_2O_7$ with $(NH_4)_2SO_4$; the other is the thermal decomposition of CrO_3. For the former process, the content of sulfur as impurity in the final product and the comprehensive utilization of the Cr(VI)-containing by-product Na_2SO_4 need to be properly resolved. For the latter process, the environmental pollution resulting from the Cr(VI)-containing dust is often serious [1].

In recent years, various processes for preparing chromic oxide green pigments with high quality have been developed with special consideration of environmental protection. Blonski et al. obtained a kind of military chromic oxide green pigment with a corundum–hematite crystalline structure, relatively low CIE-Y values, and high near-infrared reflectance [2]. Wilhelm et al. prepared a kind of chromic oxide green with low content of hexavalent chromium by adding 0.5–10.0 wt% of H_3BO_3 and H_3PO_4 [3]. Chromic oxide green with a water number of 10–40 g/100 g was prepared by Rademachers et al. through adding sulfates, polyphosphates, polyacrylates, or mixtures thereof, in quantities of from 0.1 to 2.0 wt% [4]. Muñoz et al. synthesized an environmentally friendly green pigment based on $Cr_{2-x}Al_xO_3$ solid solution with low content of Cr(VI) [5]. Berry et al. [6] and Lazău et al. [7] prepared chromic oxide green pigment from leather waste water separately.

In the 1970s, Mansmann et al. and Hahnkamm et al. proposed a hydrogen reduction method for preparing chromic oxide green pigments [8–11]. The raw materials used are hexavalent chromium (in the form of Na_2CrO_4, K_2CrO_4, $Na_2Cr_2O_7$, or $K_2Cr_2O_7$) and a salt-forming gas such as Cl_2, HCl, Br_2 or HBr. The reduction temperature is as high as 900–1600 °C, provided by combustion of hydrogen in the presence of oxygen. The process is relatively simple and high quality chromic oxide green pigments could be obtained in a single reactor. However, the valuable alkali metal, Na or K, in the raw materials is degraded to NaCl, NaBr, KCl, or KBr by-product with low value; and precision control of hydrogen and oxygen to avoid explosion poses a difficult processing problem, not to say the availability of the reactor material to withstand the highly corrosive intermediate NaOH or KOH under the high reaction temperature. Related experimental investigation has not been found in the literature.

Bai et al. proposed a new hydrogen reduction method, different from the method proposed by Mansmann et al. and Hahnkamm et al., for producing chromic oxide green to be integrated in the

* Corresponding author. Tel.: +86 10 82627096; fax: +86 10 82621022.
E-mail address: ipecas_hbxu@263.net (H.-B. Xu).

0143-7208/$ – see front matter © 2008 Elsevier Ltd. All rights reserved.
doi:10.1016/j.dyepig.2008.07.016

green metallurgical process of chromite ore [12,13]. An intermediate product in the form of CrOOH was first produced at the low temperature of 300–800 °C and an extra thermal decomposition step was provided for converting CrOOH to Cr_2O_3. This new hydrogen reduction method greatly decreased the environmental pollution resulting from Cr(VI)-containing by-products, and effectively achieved the recycling of NaOH or KOH by-product to the front end. However, the colour performance of the final Cr_2O_3 products of the new process was inferior to commercial standards, thus calling for additional measures.

This study thus aimed at improving the colour performance of the chromic oxide green product prepared through the hydrogen reduction method of Bai et al., by adopting an additional activated sintering step which incorporates Al and Ba to influence the microstructure and phase composition of Cr_2O_3 to improve its colour performance.

Colour performance was quantitatively measured in accordance to the CIE-$L^*a^*b^*$ colorimetric system, in which CIE-L^* denotes the degree of lightness and darkness of the colour in relation to the scale extending from white ($L^* = 100$) to black ($L^* = 0$), CIE-a^* denotes the scale extending from green ($-a^*$) to red ($+a^*$) axis, and CIE-b^* denotes the scale extending from blue ($-b^*$) to yellow ($+b^*$) axis.

The parameters C^* and ΔE^*_{ab} were also employed to measure the colour performance.

For commercial chromic oxide green pigment, the green colour is typically characterized as $L^* = 45$–50, $a^* < -20$, $b^* > 20$ and $C^* = 28$–30. The value of C^* is also related to the L^* value on colour effects of chromic oxide green pigments; for example, when the L^* value is close to 50, the C^* value becomes close to 30 correspondingly.

2. Experimental

K_2CrO_4 used in this work was of analytical grade manufactured by Tianjin Fu Chen Co., Ltd. of China, and the purity of the hydrogen gas used was 99.99% v/v. Gas–solid reduction was carried out in a tube furnace with a programmable temperature controller. A nickel boat, loaded with 100–150 mesh K_2CrO_4 particles, was first put into the furnace tube. Hydrogen was then introduced at a constant flow rate into the tube, while the reaction temperature was raised to and kept at about 450 °C for 1 h for the reaction to proceed, and then the furnace was let to cool naturally to ambient temperature. The reduction product was lixiviated with distilled water several times to completely remove the soluble components. The resulting intermediate was then dried at 105 °C for 12 h.

The initial samples used for sintering were doped with the above intermediates with 0, 0.25, 1.0, 2.0 wt% $Al(NO_3)_3$ and 0, 1.00, 2.00 wt% $Ba(NO_3)_2$, respectively, according to the following procedure. A required weight of $Al(NO_3)_3$ and/or $Ba(NO_3)_2$ as additive was first dissolved in a proper volume of pure water and the intermediate was then mixed with and evenly dispersed in a given volume of the aqueous solution, that is, approximately 20 mL of the aqueous solution for 100 g of the intermediate powder. Next, the wet mixtures of the intermediate powder and aqueous solution were sintered in air in an electric muffle furnace at 950 °C for 1.5 h and then quickly cooled. After sintering, the resulting powders were lixiviated with distilled water several times, vacuum dried and sieved at 45 μm.

The microstructure and morphology of the prepared Cr_2O_3 samples with different contents of Al and Ba were analyzed by Scanning Electron Microscopy (SEM). The phase of the prepared Cr_2O_3 samples was analyzed by X-ray powder diffraction (XRD) with a Rigaku Diffractometer using Cu Kα radiation.

Quantitative analysis of morphology and microstructure of the prepared Cr_2O_3 samples was carried out by FEI SIRION 200/INCA Oxford (USA/UK).

The tri-stimulus values of the CIE-$L^*a^*b^*$ parameters for the experimental Cr_2O_3 samples and standard commercial Cr_2O_3 samples were measured on an SC-80C Automatic Differential Colorimeter with an illuminant D65, and a measurement precision of ±0.01, and the colour performance data were reported in a CIE-$L^*a^*b^*$ colorimetric system. For each colorimetric parameter of a sample, three values were measured and the average value was chosen as the result. Typically, for a given sample, the standard deviation of the measured CIE-$L^*a^*b^*$ values is less than 0.10, and the relative standard deviation not higher than 0.8%, indicating that the measurement error can be ignored.

Electronic absorption spectra were measured by employing a Perkin–Elmer spectrophotometer, with a scan step of 0.5 nm in the spectral range from 400 to 800 nm using barium sulfate as a reference.

The elemental composition of the samples was measured on an Optima 5300 DV Perkin–Elmer Inductively Coupled Plasma (ICP-AES).

3. Results and discussion

3.1. Colour performance

Industrial chromic oxide green pigment Samples P1 and P2 were chosen as our standards (STD), representative of industrial production as well as colour performance. Compared to the standard samples, a more saturated green colour with a lower L^* value, lower a^* value, and higher b^* value is desirable. As can be seen from Table 1, the colour performance of Sample S1 needs to be improved

Table 1
Chemical compositions and colour performance of samples doped with different contents of Al and Ba in the initial mixture

Sample	Chemical composition (wt%)					CIE-$L^*a^*b^*$ parameters				
	Cr_2O_3	K	Al	Ba	Fe	L^*	a^*	b^*	C^*	ΔE^*_{ab}
S1	99.6	0.10	–	–	–	54.00	−21.40	18.60	28.35	5.0
S2	99.4	0.06	0.20	–	–	53.10	−21.40	21.20	30.12	3.4
S3	98.5	0.07	1.30	–	–	55.20	−20.80	16.40	26.49	7.3
S4	99.2	0.06	–	0.59	–	48.89	−21.20	18.63	28.22	2.7
S5	98.6	0.05	–	1.01	–	48.58	−18.08	18.88	26.14	4.0
S6	99.2	0.08	0.11	0.55	–	50.04	−21.95	21.41	30.66	0.8
S7	99.1	0.08	–	–	0.64	51.18	−18.98	13.27	23.16	8.4
P1[a]	99.15	–	–	–	–	50.80	−20.50	22.20	30.22	1.7
P2[b]	99.50	0.01	0.20	–	–	49.70	−21.20	21.20	30.00	0

[a] Sample P1: industrial chromic oxide green pigment from a foreign manufacturer, selected as one of the standard samples, produced by the reduction of $Na_2Cr_2O_7$ with $(NH_4)_2SO_4$.
[b] Sample P2: industrial chromic oxide green pigment from a domestic manufacturer, selected as the other standard samples, produced by the thermal decomposition of CrO_3.

by varying different contents of Al and Ba. The value of b^* increased by more than 2 when the content of Al increased from 0 to 0.20 wt%, the value of L^* decreased by more than 5 when the content of Ba increased from 0 to 0.59 wt%. The L^* and C^* values of Sample S6, which was doped with 0.1 wt% Al and 0.55 wt% Ba, were 50.04 and 30.66, respectively, very close to those of the STD. However, the colour performance worsened when excessive amounts of Al and Ba were added to the samples, that is, for Samples S3 and S5, the total CIE-$L^*a^*b^*$ values worsened when the samples were doped with 1.30 wt% of Al and 1.01 wt% of Ba, respectively.

3.2. Chemical composition and impurities

According to most international standards for commercial chromic oxide green pigment, the purity of Cr_2O_3 needs to be not lower than 99.0 wt%. As can be seen from Table 1, most samples prepared in this work meet this requirement, the Cr_2O_3 content for Sample S6 being even as high as 99.2 wt%, despite doping with Al and Ba. Addition of Al and Ba does not influence the content of some major impurities of the samples. The content of K, the most important impurity in the process, was kept below 0.1 wt% in the prepared samples. Another major impurity, Fe, should be completely removed from the samples, as shown by the C^* value of Sample S7 doped with 0.64 wt% of Fe, as low as 23.16. As can be seen in Table 2, the energy for the spin allowed transition $^4A_{2g} \rightarrow {}^4T_{1g}$ is 21 600 cm^{-1}. For Sample S7, the values of the Racah parameters B and C are 459 and 3690, respectively, obviously higher than those of the other samples such as S1, S3, and S6.

3.3. XRD

Fig. 1 shows the XRD patterns of Samples S1 (no Al or Ba), S3 (1.30 wt% Al), and S5 (1.01 wt% Ba) obtained by sintering the intermediates doped with Al and/or Ba at 950 °C for 1.5 h. Compared to Sample S1, S3 shows no other phase with its 1.30 wt% Al implying that the added Al must have entered the crystal structure of Cr_2O_3 to form a solid solution as predicted by the phase diagram of the Al_2O_3–Cr_2O_3 system [14]. For Sample S5 doped with 1.01 wt% Ba, a peak for $BaCr_2O_4$ appeared as a secondary phase which worsened the colour performance with a remarkable decrease of C^* value.

3.4. Morphology

Fig. 2 shows the morphology and EDX mapping of the samples sintered at 950 °C for 1.5 h for the same three Samples S1, S3 and S5. The morphology of all samples appeared tabular when the content of Al was less than 0.2 wt% (S2). However, the morphology became irregular and large particles appeared when the sample was doped with 1.30 wt% Al as for S3. Such large particles were found to possess higher content of Al and lower content of Cr, as well as the presence of Na, Si and Ca as impurities, as can be seen in the attached EDX of Fig. 2. Excessive content of Al thus resulted in solute segregation, change of morphology, and deterioration of colour performance.

Table 2
Values of the Racah parameters B and C and the energies (E) required for electronic transitions of Cr(III) from ground state $^4A_{2g}$

Sample	E ($^4T_{1g}$)	E ($^4T_{1g}$) = 10 Dq	E ($^2T_{1g}$)	E (^4E_g)	B	C
S1	16 600	21 550	15 100	–	462	3649
S3	16 640	21 460	15 200	–	447	3725
S6	16 670	21 460	14 680	–	444	3562
S7	16 670	21 600	15 200	–	459	3690

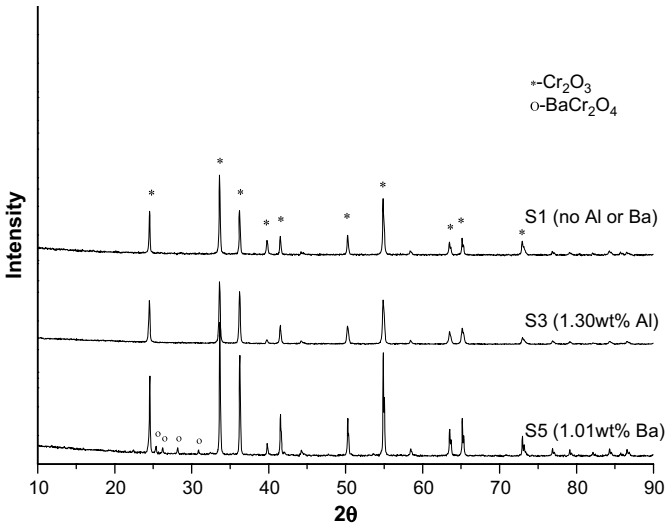

Fig. 1. XRD patterns of prepared Cr_2O_3 samples S1, S3, and S5.

The morphology of Sample S4 doped with 0.59 wt% Ba remained tabular implying that Ba must have dispersed uniformly. As a matter of fact, Ba could not be detected in Sample S4 by EDX analysis, though chemical analysis showed the content of Ba to reach 0.59 wt%, detection limit of the EDX could explain the result.

For Sample S5, doped with 1.01 wt% Ba, small massive tabular particles coexisted with large particles, and EDX mapping shows Ba to have dispersed uniformly in the small particles; though the content of Ba in the large particles is far higher than that in the small particles. XRD results show further that Cr_2O_3 coexists with a secondary phase of $BaCr_2O_4$. It can be concluded that enrichment of Ba to have taken place primarily as a secondary phase $BaCr_2O_4$ existing in the enriched areas, and that large particles are formed through co-sintering of $BaCr_2O_4$ and Cr_2O_3.

3.5. Colouring mechanism of Cr_2O_3 doped with Al and Ba

The band positions in the UV spectra are crucial for the colour perceived by human eyes. Several parameters, including the crystal field parameter Δ, and the Racah parameters B and C which can be extracted from the values of ν_1, ν_2, ν_3, can be used to characterize the electronic properties of the transition-element complexes. The crystal field parameter Δ is given by $\Delta = \nu_1$, the Racah parameter B, by $B = (2\nu_1 - \nu_2)\cdot(\nu_2 - \nu_1)/(3(9\nu_1 - 5\nu_2))$, and the Racah parameter C, by $C = (\nu_3 - 9B)/3$ [15,16].

Fig. 3 demonstrates the absorption spectra for Cr_2O_3 samples doped with Al and Ba, greater absorption in the visible region and increasing with the amounts of Al and Ba. The optical spectra of the Cr_2O_3 samples presented an intense hump above 400 nm. Two maxima of absorbance at ~450 and ~620 nm and a shoulder in the 650–700 nm range could be appreciated. The bands at ~450 and ~620 nm can be attributed to the $^4A_{2g} \rightarrow {}^4T_{1g}$ and $^4A_{2g} \rightarrow {}^4T_{2g}$ transitions of $Cr^{(III)}$ in octahedral sites, respectively [17]. These spectra exhibit the typical features of Cr(III), e.g. the bands at ~450 and ~620 nm that are observed in other pigments containing Cr(III), such as $MgCr_2O_4$, $YCrO_3$, and $YAlO_3$:0.05Cr [16,18].

As can be seen from Table 2, the spectral data led to $\Delta = 16\,600\ cm^{-1}$ for Sample S1, while the values of the Racah parameters B and C were 462 and 3649, respectively. The crystal field strength (=10 Dq) of all samples changed little. However, energy of the spin allowed transition $^4A_{2g} \rightarrow {}^4T_{1g}$ varied between 21 600 and 21 460 cm^{-1} according to the contents of Al and Ba. The absorption peaks are blue-shifted, showing increase of the b^* value. The value of the Racah parameter B varied from 462 to 444 as well.

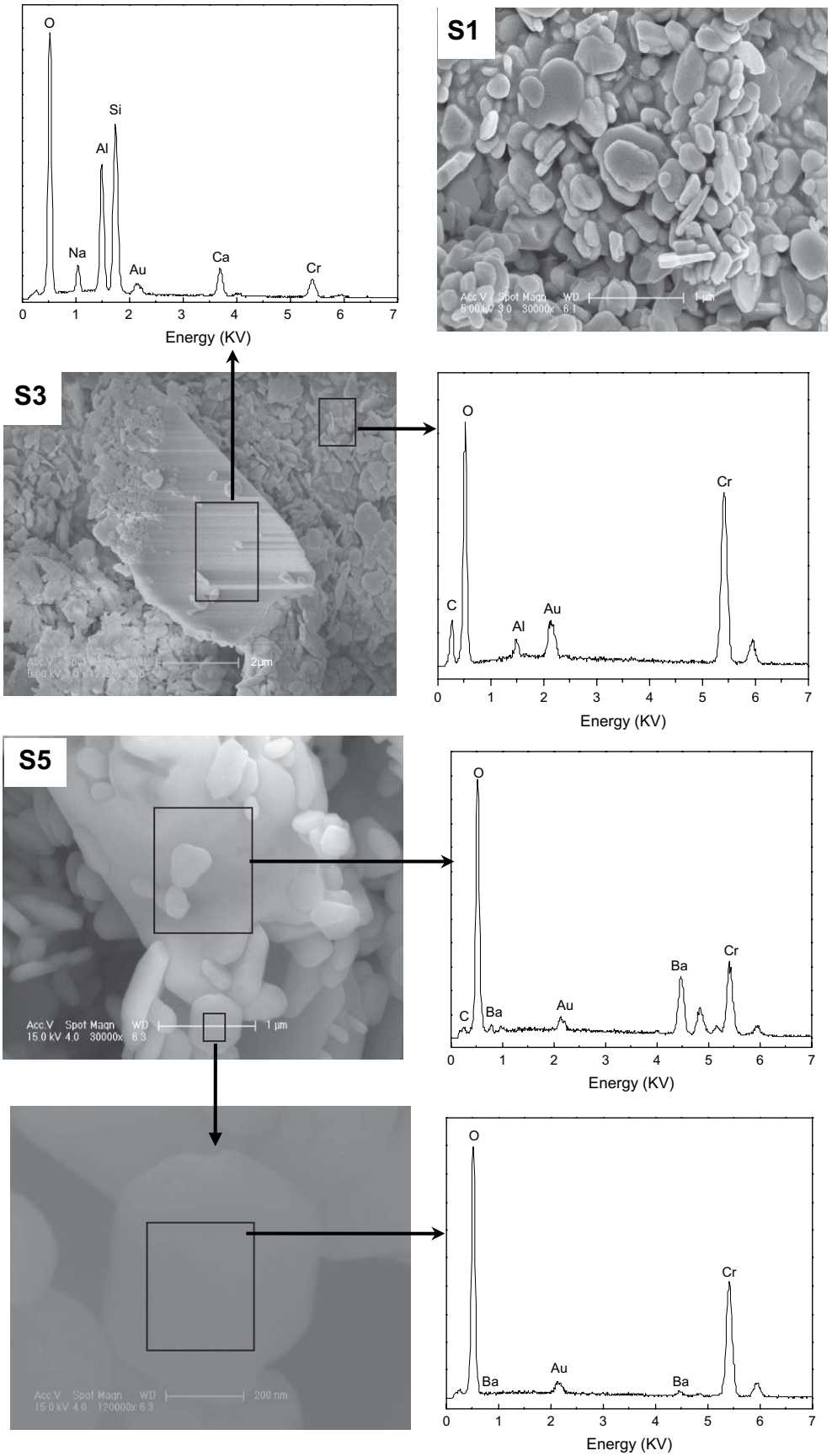

Fig. 2. SEM photographs and EDX mapping of Samples S1 (no Al and Ba), S3 (1.30 wt% Al) and S5 (1.01 wt% Ba).

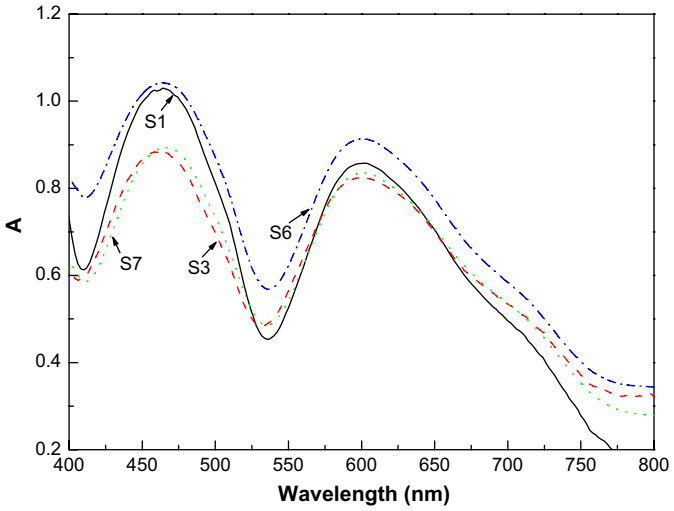

Fig. 3. UV absorption spectra for Samples S1, S3, S6, and S7.

The spectra of Sample S6 demonstrated a higher energy of the typical bands of Cr(III). The hyperchromic effect might have occurred, leading to a lower L^* value (lightness) and a higher C^* value (saturation).

The energy of the spin-forbidden transitions $^4A_{2g} \rightarrow {}^2T_{1g}$ presented little variations. It had shifted from ~15 100 cm^{-1} of sample S1 to ~14 680 cm^{-1} of sample S1. Red shift of the spectra occurred for Sample S6. Red colour was absorbed and a complimentary blue-green colour appeared.

4. Conclusions

The effects of Al and Ba on the colour performance of chromic oxide green pigment, and the phase composition and microstructure were investigated in detail, leading to the following conclusions:

(1) Excellent colour performance of chromic oxide green pigment was obtained by doping with optimal amounts of Al and Ba, that of the sample doped with 0.11 wt% Al and 0.55 wt% Ba approaching that of the commercial pigment standards.
(2) The colour performance of chromic oxide green pigment worsened when doped with excessive amount of Al and/or Ba, especially with the impurity Fe.
(3) A solid solution of Al_2O_3–Cr_2O_3 came into being and a secondary phase $BaCr_2O_4$ appeared when a chromic oxide green pigment was doped with Al and Ba, respectively. An enrichment area appeared in chromic oxide green pigment doped with excessive amounts of Al and Ba. Doping with excessive amount of Al led to solute segregation, resulting Al and other impurities were enriched. Doping with excessive amount of Ba led to large particles through co-sintering of $BaCr_2O_4$ and Cr_2O_3.
(4) When chromic oxide green pigment was doped with Al and Ba, blue shift of absorption peaks resulting from the transition $^4A_{2g} \rightarrow {}^4T_{1g}$, which helped to increase the b^* value. Hyperchromic effect and red shift of absorption peaks due to the transition $^4A_{2g} \rightarrow {}^2T_{1g}$ might also be helpful to improve the colour performance of the chromic oxide green pigment doped with Al and Ba.

Acknowledgements

The authors gratefully acknowledge the financial supports from the Knowledge Innovation Program of the Chinese Academy of Sciences (No. 082813), the National Science and Technology Pillar Program of China (No. 2006BAC02A05), and the National Basic Research Program (973 Program) of China (No. 2007CB613500). The authors are thankful to Prof. (Emeritus) Mooson Kwauk (Member of CAS) for his revision in the English language usage of this article.

References

[1] Ding Y, Ji Z. Production and utilization of chromium compounds. Beijing: Chemical Industry Press; 2003.
[2] Blonski RP, Sliwinski TR, Pipoly RA. US Patent 6,174,360 B1; 2001.
[3] Wilhelm V, Messer D. US Patent 5,167,708; 1992.
[4] Rademachers J, Rade D, Hofs H, Teichmann G, Trenczek G. US Patent 4,957,562; 1990.
[5] Muñoz R, Masó N, Julián B, Márquez F, Beltrán H, Escribano P, et al. Journal of the European Ceramic Society 2004;24(7):2087–94.
[6] Berry FJ, Costantini N, Smart LE. Waste Management 2002;22:761–72.
[7] Lazău RI, Păcurariua C, Becherescua D, Ianoş R. Journal of the European Ceramic Society 2007;27(2–3):1899–903.
[8] Mansmann M, Rambold W. US Patent 4,067,747; 1978.
[9] Mansmann M, Brandle K. British Patent 1,498,300; 1975.
[10] Hahnkamm V, Broja G, Brandle K, Elstermann CH. US Patent 3,723,611; 1973.
[11] Hahnkamm V, Broja G, Brandle K, Elstermann CH. British Patent 1,353,361; 1971.
[12] Bai YL, Xu HB, Zhang Y, Li ZH. Journal of Physics and Chemistry of Solids 2006;67(12):2589–95.
[13] Zhang Y, Li ZH, Qi T, Zheng SL, Li HQ, Xu HB. Environmental Progress 2005;24(1):44–50.
[14] Anthony RW. Solid state chemistry and its applications. John Wiley & Sons; 1984.
[15] Émilie G, Philippe S, Farid J, Federica B, Philippe O, Isabelle L. Physics and Chemistry of Minerals 2006;32:710–20.
[16] Radostin SP, Vicente BM, Juan BC. Journal of Materials Chemistry 2002;12:2825–32.
[17] Galindo R, Llusar M, Tena MA, Monros G, Badenes JA. Journal of the European Ceramic Society 2007;27:199–205.
[18] Abo-Naf SM, El-Amiry MS, Abdel-Khalek AA. Optical Materials 2008;30: 900–9.